J. Phys.: Condens. Matter **20** (2008) 275235 (6pp) doi:10.1088/0953-8984/20/27/275235

Phase coexistence and metastability in polycrystalline $Pr_{0.2}La_{0.8}Fe_{11.4}Al_{1.6}$ compound

Q Y Dong, J Chen, H W Zhang[1], J R Sun and B G Shen

State Key Laboratory of Magnetism, Institute of Physics and Centre for Condensed Matter Physics, Chinese Academy of Sciences, Beijing 100080, People's Republic of China

E-mail: hwzhang@aphy.iphy.ac.cn

Received 6 March 2008, in final form 14 May 2008
Published 6 June 2008
Online at stacks.iop.org/JPhysCM/20/275235

Abstract

Electrical resistivity, dc magnetization, ac magnetic susceptibility, and magnetic relaxation studies of polycrystalline $Pr_{0.2}La_{0.8}Fe_{11.4}Al_{1.6}$ compound have been carried out. On the basis of the measurements of isofield magnetization and ac magnetic susceptibility, we provide evidence for phase coexistence (the appearance of the ferromagnetic phase in the antiferromagnetic matrix) rather than a spin glass, resulting in a cusp observed at ∼70 K in the zero-field-cooled thermal magnetization curve under low fields. The ferromagnetic clusters or nuclei appear randomly in the antiferromagnetic matrix according to the electrical resistivity results. An excellent magnetic–resistive correspondence is observed under medium fields. Under these fields large relaxation effects are presented in the vicinity of the phase transition temperature. Nonuniform variation of the relaxation rate with temperature gives a clear picture of the nucleation and growth of phases. Distinct metastable behavior is shown during the phase transition, which brings about the step-like behavior in the various magnetization curves.

(Some figures in this article are in colour only in the electronic version)

1. Introduction

In $LaFe_{13-x}Al_x$ compounds crystallizing in the cubic $NaZn_{13}$-type structure, an antiferromagnetic (AFM) state is established in the concentration range $1.04 \leqslant x \leqslant 1.69$ [1, 2]. A large magnetocaloric effect, remarkable magnetovolume effect and large magnetoresistance effect have been observed, which are caused by an itinerant-electron metamagnetic transition, i.e. the magnetic-field-induced first-order transition [3–5]. Despite this progress, the nature of the AFM structure is not immediately clear because no simple AFM lattice can be mapped on the $NaZn_{13}$-type crystal structure. In the $NaZn_{13}$-type structure, 96(i) sites are occupied by 12 Fe^{II} + Al atoms and the centered 8(b) site is only occupied by one Fe^{I} atom [2, 6]. With the help of neutron scattering and Mössbauer spectroscopy, one possible model of the AFM state was suggested [6]. That is, ferromagnetic (FM) clusters composed of 12 Fe^{II} + Al plus Fe^{I} are ferromagnetically coupled in the (100) plane and the interplane coupling is AFM. Nevertheless, it is difficult to understand the different characteristics of the exchange coupling because the Fe–Fe distances within a cluster are as large as those between the clusters. Furthermore, the AFM ground state can be easily transformed into the FM state by increasing the Fe concentration, introducing interstitial atoms and substituting Fe with Co and La with Nd or Pr [1, 7–12]. Therefore, more attention should be paid to the AFM ground state of $LaFe_{13-x}Al_x$ compounds.

$LaFe_{11.4}Al_{1.6}$, a member of the series, has the AFM ground state. As the replacement of La with Pr increases, the magnetic ground state is gradually changed from the AFM to the FM state [12]. Due to the introduction of Pr–Pr and Pr–Fe FM interactions into the AFM $LaFe_{11.4}Al_{1.6}$ compound, the $Pr_{0.2}La_{0.8}Fe_{11.4}Al_{1.6}$ compound shows a very interesting magnetic phase transition [12] similar to those in the Gd_5Ge_4 compound [13–18], Ru-doped $CeFe_2$ alloys [19], and Nd_7Rh_3 [20]. It orders antiferromagnetically at ∼188 K. The AFM order is sustained at least down to 5 K under magnetic fields lower than ∼4 kOe. The AFM state can

[1] Author to whom any correspondence should be addressed.

be partially or completely transformed into the FM state depending on the temperature and the applied magnetic field as long as the latter exceeds ∼4 kOe. Coexistence of the AFM and FM phase is observed under medium fields. Below ∼70 K, the magnetic-field-induced AFM–FM transition is irreversible, while above ∼85 K the transition becomes completely reversible. Between ∼70 and ∼85 K, there exists a mixture of states exhibiting both irreversible and reversible AFM–FM transitions.

In [12], the preliminary H–T magnetic phase diagram has been determined for $Pr_{0.2}La_{0.8}Fe_{11.4}Al_{1.6}$. However, some features, including the cusp in the zero-field-cooled magnetization (M) versus T curve under a low field and the thermal irreversibility of magnetic properties at low temperatures under magnetic fields less than 15 kOe have not been intensively investigated. The nature of the magnetic phase transitions is yet to be unveiled. The investigation of phase coexistence across the transition is lacking in $LaFe_{13-x}Al_x$ compounds, although work has been done in several other materials such as Gd_5Ge_4 [18], $Ce(Fe_{0.96}Ru_{0.04})_2$ [21] and Nd_7Rh_3 [22]. Thus it will be very meaningful to investigate the character of the $Pr_{0.2}La_{0.8}Fe_{11.4}Al_{1.6}$ compound in more detail. Furthermore, metastability is a characteristic feature associated with the AFM–FM transition in both Gd_5Ge_4 [15] and the doped $CeFe_2$ [19] alloys. Magnetization relaxation measurements reveal important aspects of nucleation and growth of phases across the first-order AFM–FM transition in doped $CeFe_2$ alloys [19]. In this paper we present the results of the isofield and isothermal magnetizations, frequency dependent ac magnetic susceptibility, electrical resistivity and magnetic relaxation in polycrystalline $Pr_{0.2}La_{0.8}Fe_{11.4}Al_{1.6}$. The above-mentioned cusp is caused by the coexistence of the AFM phase and FM clusters rather than the appearance of a spin glass. The results of magnetic relaxation measurements highlight the metastability of phases during the AFM and FM phase transitions. Interestingly, the step-like behavior is found in some M versus time curves.

2. Experimental details

The $Pr_{0.2}La_{0.8}Fe_{11.4}Al_{1.6}$ compound was prepared by arc melting a stoichiometric mixture of the constituent elements Pr, La, Fe and Al with purities higher than 99.9%. The ingot was vacuum annealed at 1223 K for 13 days. A nearly single $NaZn_{13}$-type phase in the sample was confirmed by x-ray diffraction.

Magnetic measurements were performed on a commercial physical properties measurement system (PPMS; Quantum Design). Three experimental protocols, zero-field-cooled (ZFC), field-cooled-cooling (FCC), and field-cooled-warming (FCW) were used for the dc magnetization measurements under the desired magnetic fields [18]. In the ZFC mode the sample was cooled to 5 K before the measuring field H was switched on and the measurement was made while warming up the sample. The applied H was switched on in the T regime above the AFM–paramagnetic (PM) transition temperature (T_N) in the FCC mode and the measurement was made when cooling across T_N. On reaching 5 K in the FCC mode, the data were taken again in the presence of the same H while warming up the sample. This was the FCW mode. The isothermal ZFC M–H curve at $T = 65$ K was measured. The magnetic relaxation behaviors were investigated at different temperatures under some typical fields. Measurements of ac magnetic susceptibility versus temperature were carried out at several frequencies (50, 1000, 3000 and 10 000 Hz) on warming up the sample, and the amplitude of the alternating field was 10 Oe. Note that each measurement sequence was recorded after a thermal demagnetization above 200 K (higher than its T_N). Electrical resistivity measurements were done using a conventional four-probe method on heating, using the temperature and magnetic field conditions of the commercial MPMS-7 superconducting quantum interference device (SQUID) magnetometer.

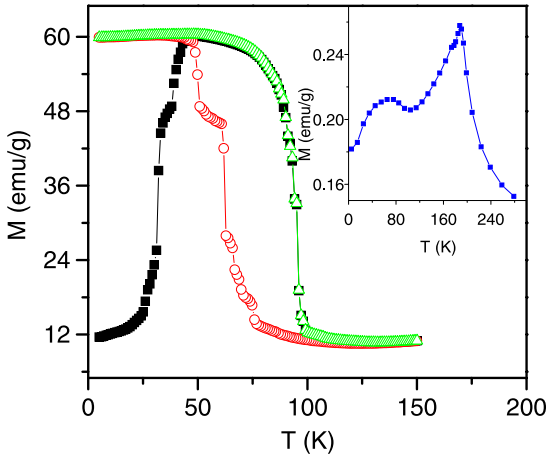

Figure 1. M versus T plots for $Pr_{0.2}La_{0.8}Fe_{11.4}Al_{1.6}$ obtained in ZFC (closed squares), FCC (open circles) and FCW (open triangles) modes under an applied H of 4.5 kOe. T is varied with a sweep rate of 2 K min^{-1}. The inset shows the ZFC $M(T)$ curve under 0.1 kOe.

3. Results and discussion

The ZFC, FCC and FCW temperature dependence of magnetization under a field of 4.5 kOe are shown in figure 1. The inset of figure 1 illustrates the ZFC temperature dependence of magnetization under $H = 0.1$ kOe with an AFM-to-PM transition at T_N (∼188 K) and a cusp at ∼70 K. When the applied field is equal to 4.5 kOe, the cusp observed around 70 K in ZFC $M(T)$ data is no longer seen. However, a plateau centered at this temperature develops, revealing the mixture of AFM and FM phases. That is, the ZFC $M(T)$ data under $H = 4.5$ kOe show that there is an AFM-to-FM transition around 32 K followed by a FM-to-AFM transition around 93 K on heating. The FCW $M(T)$ curve is very different from the ZFC one at low temperature (see figure 1). For the FCW $M(T)$ curve just above 50 K, there is a ∼30 K thermal hysteresis compared with the FCC one, which is a typical characteristic of a magnetic first-order phase transition. Interestingly, multi-step discontinuous jumps are shown across the phase transitions in the ZFC, FCC and FCW $M(T)$ curves. Similar features have also been observed under a field of 10 kOe (see figure 2). Comparing the magnetic behavior shown

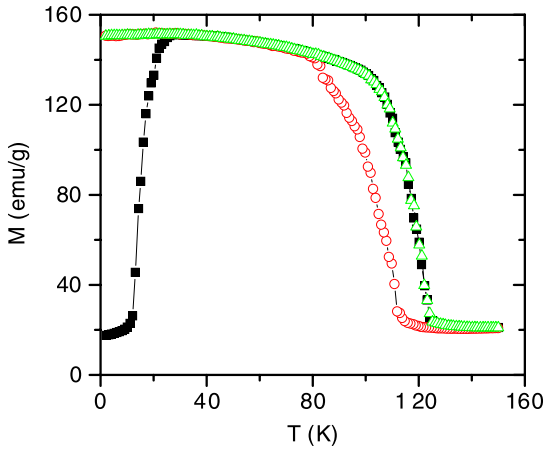

Figure 2. M versus T plots for $Pr_{0.2}La_{0.8}Fe_{11.4}Al_{1.6}$ obtained in ZFC (closed squares), FCC (open circles) and FCW (open triangles) modes under an applied H of 10 kOe. T is varied with a sweep rate of 2 K min^{-1}.

in figure 2 with that in figure 1, the differences are as follows: firstly, both the height and the width of the plateau increase greatly, which is in accord with the results in [12]; secondly, the thermal hysteresis between the FCW and FCC $M(T)$ curves decreases distinctly. Lastly, the step-like behavior almost disappears under a field of 10 kOe.

It is generally accepted that frustration or disorder are necessary to achieve a spin-glass state. The competition of various magnetic interactions may result in the appearance of a spin-glass state [23, 24]. As observed above, the competition between AFM and FM order is strong in $Pr_{0.2}La_{0.8}Fe_{11.4}Al_{1.6}$. Thus, spin-glass or cluster-glass behavior may occur. To clarify whether the cusp at ∼70 K, shown in figure 1, is an indication of the appearance of a spin glass, an ac magnetic susceptibility measurement was performed. Figure 3 shows the temperature dependence of the real part (χ') and imaginary part (χ'') of the ac magnetic susceptibility, measured under a zero external dc magnetic field at some typical frequencies. There is a broadened peak at ∼70 K. This is in accord with the cusp shown in the inset of figure 1. A close-up view of the real part around 70 K is displayed in the inset of figure 3(a). No frequency dependence of the peak position could be observed. The frequency sensitivity of the peak is used as a possible distinguishing criterion for the presence of a spin-glass state [25]. Therefore, the appearance of a spin glass should be ruled out in this sample. Similar results have been reported in Ge_5Ge_4 [16] and Nd_7Rh_3 [15].

Simultaneously, the nonzero values of χ'' indicate the onset of an energy loss process, usually associated with domain dynamics, which is consistent with weak ferromagnetism [26]. χ'' exhibits a peak at ∼70 K, although the peak is not very sharp. Thus, we can deduce that ferromagnetism occurs in the sample at ∼70 K [25]. A similar result supported by *in situ* x-ray powder diffraction study has been found in Gd_5Ge_4 [17]. One of the possible explanations is that at ∼70 K formation of a ferromagnetic nucleus takes place for the AFM-to-FM phase transition.

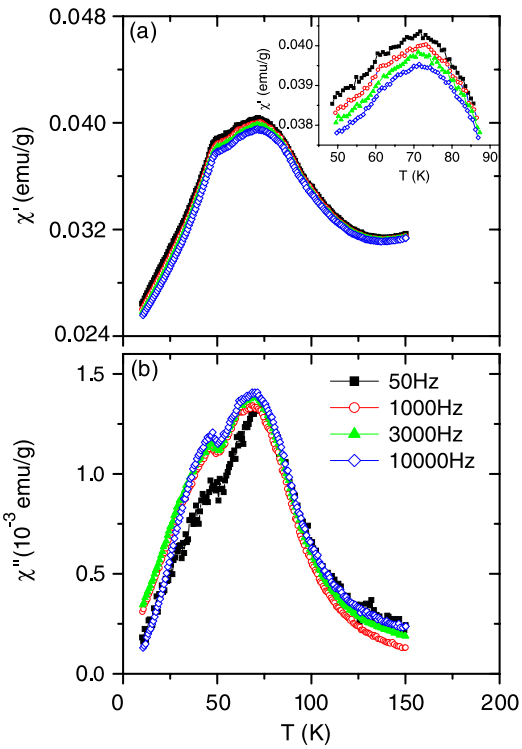

Figure 3. Temperature variation of the real (a) and imaginary (b) components of the ac susceptibility of $Pr_{0.2}La_{0.8}Fe_{11.4}Al_{1.6}$, measured under a zero external dc magnetic field at different frequencies during heating of the sample. The inset in (a) clarifies details of the real component of the ac susceptibility around 70 K. T is varied with a sweep rate of 0.25 K min^{-1}.

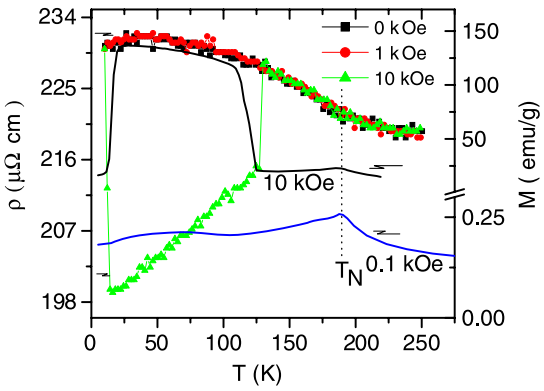

Figure 4. The variation of electrical resistivity and the corresponding magnetization of $Pr_{0.2}La_{0.8}Fe_{11.4}Al_{1.6}$ with temperature under different applied fields while warming. The Néel temperature, T_N, is marked.

The electrical resistivity (ρ) of $Pr_{0.2}La_{0.8}Fe_{11.4}Al_{1.6}$ has been measured in the temperature range of 10–250 K under fields of 0, 1 and 10 kOe on the ZFC path (see figure 4). The resistivity in the paramagnetic state is about 220 $\mu\Omega$ cm at 250 K, which is slightly larger than that of $LaFe_{11.4}Al_{1.6}$ [1]. Under a zero field the resistivity increases as the temperature drops, and it exhibits a slope change near T_N. At low temperature it shows a maximum, as often reported in AFM materials [27]. Under a field of 1 kOe, the temperature

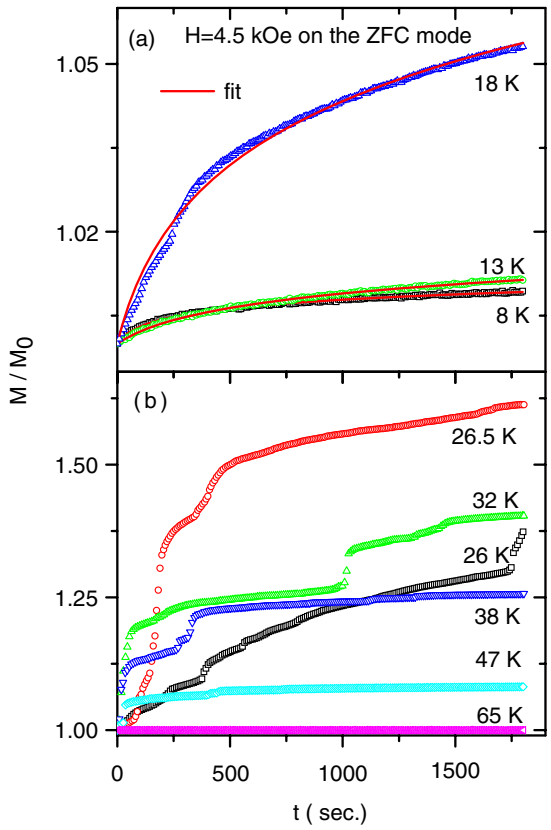

Figure 5. Normalized magnetization versus time (t) for $Pr_{0.2}La_{0.8}Fe_{11.4}Al_{1.6}$ measured at typical temperatures under $H = 4.5$ kOe in the ZFC mode. The solid line is a fit based on equation (1). At each T, M_0 is the value of the magnetization recorded when the relaxation measurements were started, i.e. 0 s after the target H and T values were reached.

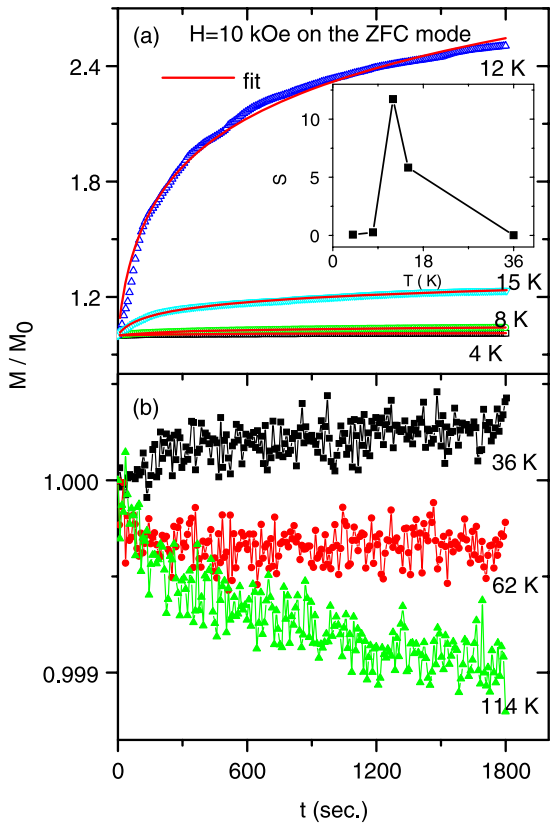

Figure 6. Normalized magnetization versus time (t) for $Pr_{0.2}La_{0.8}Fe_{11.4}Al_{1.6}$ measured at typical temperatures under $H = 10$ kOe in the ZFC mode. The solid line is a fit based on equation (1). At each T, M_0 is the value of the magnetization recorded when the relaxation measurements were started, i.e. 0 s after the target H and T values were reached. The inset in (a) shows the temperature dependence of the magnetic viscosity S, obtained based on equation (1).

dependence of the resistivity is similar to that under a zero field. Thus, the appearance of a FM phase in the AFM matrix does not affect the resistivity. That is to say, the amount of FM phase is very small and the FM phase is dispersed randomly in the AFM matrix. However, under a field of 10 kOe, the resistivity suddenly decreases with increasing temperature, at which the AFM-to-FM transition takes place. Then, the resistivity increases linearly with further increasing temperature and it shows a sudden increase at the FM-to-AFM transition temperature. Namely, a good magnetic–resistive correspondence is observed as shown in figure 4. This can be explained by using the two-current model [1]: the resistivity is largest in the AFM state, smallest in the FM state and in between in the PM state.

Figure 5 presents normalized M versus time (t) plots under $H = 4.5$ kOe at various T ($T \leqslant 71$ K) on the ZFC path. The relaxations in M as expected in [16] are exhibited at low temperature (see figure 5(a)). These $M(t)$ curves are well adjusted with a logarithmic function [28]

$$M(t) = S(T)\ln(t/t_0 + 1) + M_0, \qquad (1)$$

from which the magnetic viscosity S is extracted. The value of S changes from 0.03 at 8 K to 0.26 at 18 K. At temperatures lower than 8 K, the system is frozen in its AFM state, i.e. $S(T) \approx 0$. Strong relaxation effects in M are found between 26 and 47 K. Interestingly, M varies discontinuously at these temperatures (see figure 5(b)). At high temperatures (for example, 65 K), no thermal relaxation was observed within our experimental resolution, which illustrates that the fraction of FM state has nearly reached the saturated value.

Figure 6 presents normalized M versus time (t) plots under $H = 10$ kOe at different T on the ZFC path. The relaxation effects are found in the temperature range of 4–36 K (see figure 6(a)). $M(t)$ changes continuously and can be well fitted by equation (1). The temperature dependence of S is plotted in the inset of figure 6(a). As the temperature increases, the thermal activation energy becomes large enough to allow the system to overcome the energy barriers (that may be caused by the surface energy between the nucleated seed and the host crystal.) and thermally activate the AFM-to-FM transition. Consequently, the FM phase fraction shows a substantial growth as a function of time, and the magnetic relaxation rate increases. So an increase in S with increasing temperature is observed, as shown in figure 6(a). When the majority of the system becomes unblocked, a peak in $S(T)$ is observed. At 62 K, no obvious relaxations are observed within our experimental resolution, namely $S \approx 0$. On

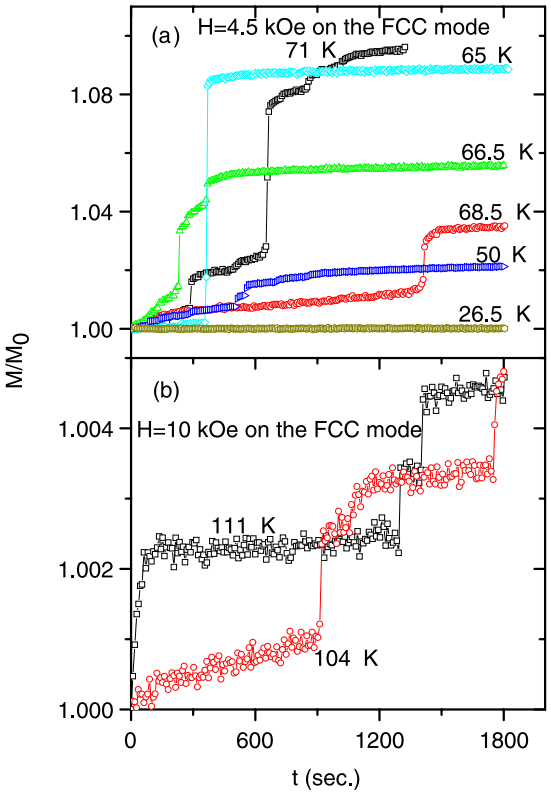

Figure 7. Normalized magnetization versus time (t) for $Pr_{0.2}La_{0.8}Fe_{11.4}Al_{1.6}$ measured at typical temperatures under (a) $H = 4.5$ kOe and (b) $H = 10$ kOe in the FCC mode. At each T, M_0 is the value of the magnetization recorded when the relaxation measurements were started, i.e. 0 s after the target H and T values were reached.

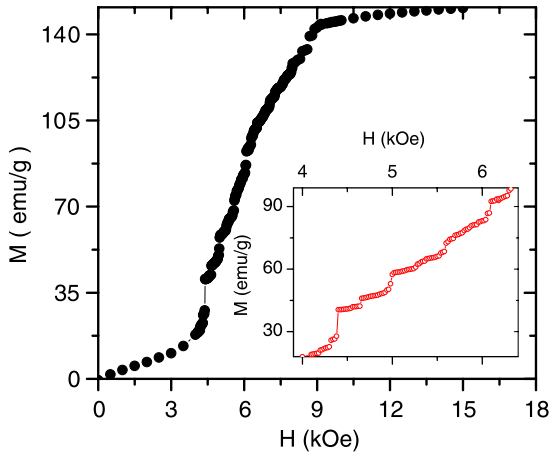

Figure 8. Isothermal variation of the magnetization for $Pr_{0.2}La_{0.8}Fe_{11.4}Al_{1.6}$ with the applied magnetic field at $T = 65$ K. The plot in the inset is an expanded view of the step-like behavior between 4.0 and 6.3 kOe.

the contrary, at 114 K a small decrease in M is observed, which indicates that at this temperature the FM state instead of the AFM one becomes metastable and then the FM-to-AFM transition rather than the AFM-to-FM one is thermally activated (see figure 6(b)).

Quite different from the results on the ZFC path, M shows an obvious relaxation between $T = 71$ and 50 K under $H = 4.5$ kOe on the FCC path. At temperatures below 50 K, no apparent decay in M is shown (see figure 7(a)). Under $H = 10$ kOe, small relaxations in M are observed at $T = 111$ and 104 K on the FCC path (see figure 7(b)).

On the one hand, some $M(t)$ curves, as shown in figures 5 and 6, can be well fitted with equation (1), which is expected in terms of thermal activation for a first-order phase transition [12, 28, 29]. The logarithmic rather than exponential dependence of M on t indicates that there is a distribution of energy barriers in the sample. On the other hand, some $M(t)$ curves as exhibited in figures 5–7 show a step-like behavior. Note that the temperature fluctuation during the measurements is controlled to be below 0.01 K and the magnetic field fluctuation can also be neglected. So we may rule out the possibility that the temperature or field fluctuation triggers the phase transition and leads to the discontinuous variation of M as shown in figures 5–7. This step-like feature can also be found in isothermal M–H curves. Figure 8 shows the ZFC isothermal M–H curves obtained at $T = 65$ K where the relaxation effect is strong in the FCC mode. Note that distinct step-like features are observed on careful inspection, as shown in the enlarged part of the M–H curve in figure 8. Similar steps in the M–H curves across the metamagnetic transition and the associated metastability have been reported in CMR manganites [30] and Gd_5Ge_4 [15]. The step-like behaviors in the M–H curves as well as in the M–t curves may reflect an avalanche-like behavior similar to the reported avalanche-like nucleation and growth of martensitic domains [31]. The broadening of the first-order phase transition as shown in figure 8 may be caused by the distribution of the local transition field across the physical dimension of the sample [15], which is coincident with the results obtained from the logarithmic dependence of M on t.

4. Summary and conclusions

The results of thermal magnetization and ac susceptibility curves illustrate that the cusp at ~70 K observed in the low field ZFC M–T curves is associated with the appearance of ferromagnetism in the AFM matrix. The electrical resistivity data prove that the resistance of the FM phase is smaller than that of the AFM phase. The amount of FM phase is very small and the FM phase is dispersed randomly in the AFM matrix under a low field. The large magnetic relaxation in M during the phase transitions reflects the distribution of energy barriers to the phase transition. The step-like behavior observed in M–t and M–H curves may reflect an avalanche-like nucleation and growth of martensitic domains.

Acknowledgments

The work was supported by the State Key Project of Fundamental Research and the National Natural Science Foundation (no. 10774178) of China.

References

[1] Plastra T T M, Nieuwenhuys G J, Mydosh J A and Buschow K H J 1984 *J. Appl. Phys.* **55** 2367
[2] Plastra T T M, Nieuwenhuys G J, Mydosh J A and Buschow K H J 1985 *Phys. Rev.* B **31** 4622
[3] Hu F X, Shen B G, Sun J R, Pakhomov A B, Wong C Y, Zhang X X, Zhang S Y, Wang G J and Cheng Z H 2001 *IEEE Trans. Magn.* **37** 2328
[4] Hu F X, Wang G J, Wang J, Sun Z G, Dong C, Chen H, Zhang X X, Sun J R, Cheng Z H and Shen B G 2002 *J. Appl. Phys.* **91** 7836
[5] Irisawa K, Fujita A, Fukamichi K, Yamada M, Mitamura H, Goto T and Koyama K 2004 *Phys. Rev.* B **70** 214405
[6] Helmholdt R B, Palstra T T M, Nieuwenhuys G J, Mydosh J A, van der Kraan A M and Buschow K H J 1986 *Phys. Rev.* B **34** 169
[7] Irisawa K, Fujita A, Fukamichi K, Yamazaki Y, Iijima Y and Matsubara E 2000 *J. Alloys Compounds* **316** 70
[8] Wang F, Chen Y F, Wang G J, Sun J R and Shen B G 2004 *J. Phys.: Condens. Matter* **16** 2103
[9] Zhang H W, Chen J, Liu G J, Zhang L G, Sun J R and Shen B G 2006 *Phys. Rev.* B **74** 212408
[10] Hu F X, Shen B G, Sun J R and Cheng Z H 2001 *Phys. Rev.* B **64** 012409
[11] Liu G J, Sun J R, Zhao T Y and Shen B G 2006 *Solid State Commun.* **140** 45
[12] Chen J, Zhang H W, Zhang L G, Sun J R and Shen B G 2007 *J. Appl. Phys.* **102** 113905
[13] Levin E M, Gschneidner K A Jr and Pecharsky V K 2002 *Phys. Rev.* B **65** 214427
[14] Pecharsky V K, Holm A P, Gschneidner K A Jr and Rink R 2003 *Phys. Rev. Lett.* **91** 197204
[15] Chattopadhyay M K, Manekar M A, Pecharsky A O, Pecharsky V K, Gschneidner K A Jr, Moore J, Perkins G K, Bugoslavsky Y V, Roy S B, Chaddah P and Cohen L F 2004 *Phys. Rev.* B **70** 214421
[16] Tang H, Pecharsky V K, Gschneidner K A Jr and Pecharsky A O 2004 *Phys. Rev.* B **69** 064410
[17] Mudryk Y, Holm A P, Gschneidner K A Jr and Pecharsky V K 2005 *Phys. Rev.* B **72** 064442
[18] Roy S B, Chattopadhyay M K, Chaddah P, Moore J D, Perkins G K, Cohen L F, Gschneidner K A Jr and Pecharsky V K 2006 *Phys. Rev.* B **74** 012403
[19] Chattopadhyay M K, Roy S B, Nigam A K, Sokhey K J S and Chaddah P 2003 *Phys. Rev.* B **68** 174404
[20] Tsutaoka T, Nakamori Y, Tokunaga T, Kadomatsu H and Itoh Y 1998 *J. Alloys Compounds* **270** 53
[21] Chattopadhyay M K, Roy S B and Chaddah P 2005 *Phys. Rev.* B **72** 180401
[22] Sengupta K and Sampathkumaran E V 2006 *Phys. Rev.* B **73** 020406
[23] Fischer K H 1975 *Phys. Rev. Lett.* **34** 1438
[24] Binder K and Yong A P 1986 *Rev. Mod. Phys.* **58** 801
[25] Wang F, Zhang J, Chen Y F, Wang G J, Sun J R, Zhang S Y and Shen B G 2004 *Phys. Rev.* B **69** 094424
[26] Ouyang Z W, Pecharsky V K, Gschneidner K A Jr, Schlagel D L and Lograsso T A 2006 *Phys. Rev.* B **74** 094404
[27] Irisawa K, Fujita A, Fukamichi K, Mitamura H and Goto T 2001 *J. Alloys Compounds* **327** 17
[28] Ghivelder L and Parish F 2005 *Phys. Rev.* B **71** 184425
[29] Zhang H W, Wang F, Zhao T Y, Zhang S Y, Sun J R and Shen B G 2004 *Phys. Rev.* B **70** 212402
[30] Wu T and Mitchell J F 2004 *Phys. Rev.* B **69** 100405
[31] Perez-Reche F J, Stipcich M, Vives E, Manosa L, Planes A and Morin M 2004 *Phys. Rev.* B **69** 064101